CHEMISTRY OF MATERIALS

Article

pubs.acs.org/cm

Probing Eu^{2+} Luminescence from Different Crystallographic Sites in $Ca_{10}M(PO_4)_7:Eu^{2+}$ (M = Li, Na, and K) with β-$Ca_3(PO_4)_2$-Type Structure

Mingyue Chen,[†] Zhiguo Xia,*[,†] Maxim S. Molokeev,[‡,∥,⊥] Chun Che Lin,[#] Chaochin Su,[#] Yu-Chun Chuang,[§] and Quanlin Liu[†]

[†]The Beijing Municipal Key Laboratory of New Energy Materials and Technologies, School of Materials Sciences and Engineering, University of Science and Technology Beijing, Beijing 100083, China

[‡]Laboratory of Crystal Physics, Kirensky Institute of Physics, Federal Research Center KSC SB RAS, Krasnoyarsk 660036, Russia

[∥]Siberian Federal University, Krasnoyarsk 660041, Russia

[⊥]Department of Physics, Far Eastern State Transport University, Khabarovsk 680021, Russia

[#]Institute of Organic and Polymeric Materials, National Taipei University of Technology, Taipei 106, Taiwan

[§]National Synchrotron Radiation Research Center, Hsinchu 300, Taiwan

Supporting Information

ABSTRACT: Eu^{2+} local environments in various crystallographic sites enable the different distributions of the emission and excitation energies and then realize the photoluminescence tuning of the Eu^{2+} doped solid state phosphors. Herein we report the Eu^{2+}-doped $Ca_{10}M(PO_4)_7$ (M = Li, Na, and K) phosphors with β-$Ca_3(PO_4)_2$-type structure, in which there are five cation crystallographic sites, and the phosphors show a color tuning from bluish-violet to blue and yellow with the variation of M ions. The difference in decay rate monitored at selected wavelengths is related to multiple luminescent centers in $Ca_{10}M(PO_4)_7:Eu^{2+}$, and the occupied rates of Eu^{2+} in Ca(1), Ca(2), Ca(3), Na(4), and Ca(5) sites from Rietveld refinements using synchrotron power diffraction data confirm that Eu^{2+} enters into four cation sites except for Ca(5). Since the average bond lengths d(Ca−O) remain invariable in the $Ca_{10}M(PO_4)_7:Eu^{2+}$, the drastic changes of bond lengths d(M−O) and Eu^{2+} emission depending on the variation from Li to Na and K can provide insight into the distribution of Eu^{2+} ions. It is found that the emission band at 410 nm is ascribed to the occupation of Eu^{2+} in the Ca(1), Ca(2), and Ca(3) sites with similar local environments, while the long-wavelength band (466 or 511 nm) is attributed to Eu^{2+} at the M(4) site (M = Na and K). We show that the crystal-site engineering approach discussed herein can be applied to probe the luminescence of the dopants and provide a new method for photoluminescence tuning.

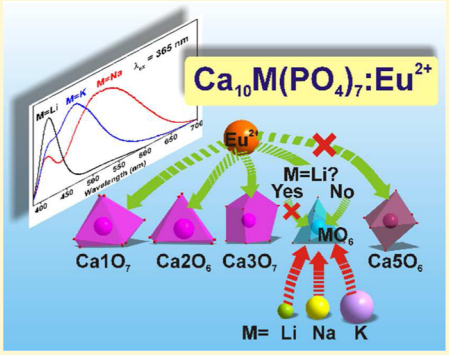

INTRODUCTION

Rare earth (RE)-activated luminescent materials with widely and continuously tunable excitation and emission wavelength are of considerable interest due to their applications in light emitting diode (LED)-based solid-state lighting.[1,2] To target phosphor-converted LEDs with specific photoluminescence properties, vigorous investigations have been performed on the different host systems, such as nitrides, fluorides, silicates, phosphates, and so on.[3−5] Among them, whitlockite β-$Ca_3(PO_4)_2$ host has been studied in recent years due to its versatile structural types as well as the tunable luminescence behaviors doped with rare earth.[6,7] The β-$Ca_3(PO_4)_2$ host possesses five independent cationic crystallographic sites named Ca(1), Ca(2), Ca(3), Ca(4), and Ca(5), and the coordination numbers are seven for Ca1, eight for Ca2, eight for Ca3, three for Ca4, and six for Ca5.[1] The Ca(1), Ca(2), Ca(3), and Ca(5) sites are 100% occupied by Ca^{2+} ions, but the Ca(4) site is occupied by 50% Ca^{2+} ions and 50% vacancies.[8] Based on the specific crystal structure of β-$Ca_3(PO_4)_2$, many new hosts with β-$Ca_3(PO_4)_2$-type structure can be constructed through ion substitution. Partial substitution of Ca^{2+} by Sr^{2+} ($Ca_{3-x}Sr_x(PO_4)_2$) results in a phase transition ($\beta \rightarrow \beta'$)[9] and a red-shifted Eu^{2+} emission.[8] Furthermore, a new yellow-emitting $Sr_{1.75}Ca_{1.25}(PO_4)_2:Eu^{2+}$ phosphor was found and applied to near-ultraviolet (UV) light pumped white LEDs.[10] The Ca^{2+} also can be replaced by monovalent M^+ and trivalent R^{3+}, and this substitution yielded a large number of new hosts with β-$Ca_3(PO_4)_2$-type structure, such as $Ca_{10}M(PO_4)_7$ (M = Li, Na, and K),[11−14] $Ca_9R(PO_4)_7$ (R = Cr and Rare earth),[15−18] $Ca_8MgLn(PO_4)_7$ (Ln = Y, La),[19−21] and so on. Among these, the Eu^{2+} doped $Ca_9Lu(PO_4)_7$ phosphor shows a broad blue-green emission band (480 nm),[22] and the emission band of $Ca_9Y(PO_4)_7:Eu^{2+},Mn^{2+}$ can be tuned from 486 to 638 nm through energy transfer from Eu^{2+} to Mn^{2+}.[23]

Generally, a solid state compound involving two or more sites, which luminescent center ions (such as Eu^{2+}, Ce^{3+}) can

Received: June 30, 2017
Revised: August 4, 2017
Published: August 7, 2017

DOI: 10.1021/acs.chemmater.7b02724
Chem. Mater. 2017, 29, 7563−7570

occupy, will be challenging for photoluminescence tuning.[24] The Eu^{2+} emission changes greatly depending on the local environment of Eu^{2+} in different sites, which is called crystal-site engineering.[25,26] As an example of Ca_2SiO_4:Eu^{2+}, Eu^{2+} with low doping level prefers occupying the Ca(1*n*) sites corresponding to green-yellow emission, and for higher Eu^{2+} content, the red emission could be assigned to the Eu^{2+} in the Ca(2*n*) sites.[25] Based on these results, for the β-$Ca_3(PO_4)_2$ structure, there are five different crystallographic sites for $Eu^{2+}$to occupy, which should lead to different Eu^{2+} luminescences. Actually, in our previous work,[27] we found Eu^{2+} occupied four sites corresponding to two groups of emission bands. Moreover, we gave the relationships between the distribution of Eu^{2+} in four sites and the luminescent property. It was proposed that the short-wavelength emission band was ascribed to the Eu^{2+} ions occupied over Ca(1), Ca(2), and Ca(3) sites, and these three sites have the same point symmetry *C*1, while the long-wavelength emission band was owing to the Eu^{2+} ions entering the 6-fold coordination M(4) site with point symmetry *C*3.[27] In $Ca_{10}Na(PO_4)_7$:Eu^{2+}, Yu et al. considered that there are also four luminescence centers, but they result from Eu^{2+} entering into the Ca(1), Ca(2), Ca(3), and Ca(5) sites.[28] The structure of $Ca_{10}Na(PO_4)_7$ was not clear, and even the Na(4) site was not mentioned. Furthermore, Liu et al. reported the structure of $Ca_{10}K(PO_4)_7$:Eu^{2+} phosphor and found that the size of K^+ was too large to be normally replaced by Eu^{2+} ions. The broad band was also attributed to Eu^{2+} occuping the Ca(1), Ca(2), Ca(3), and Ca(5) randomly, which was corresponding to 460, 489, 544, and 600 nm.[29] The above results for Eu^{2+} luminescence from the Ca(1), Ca(2), Ca(3), and Ca(5) sites are not consistent with our proposed model that the different luminescent behaviors are due to the distribution of Eu^{2+} in the Ca(1), Ca(2), Ca(3), and M(4) sites.

Therefore, to probe the relationship between Eu^{2+} luminescence and the different distributions of Eu^{2+} in diverse sites and confirm to which crystallographic site for Eu^{2+} the emission band belongs, we design the $Ca_{10}M(PO_4)_7$:Eu^{2+} (M = Li, Na and K) and investigate Eu^{2+} emission depending on the variation from Li to Na to K ions. The variation in decay rate with respect to different detection wavelengths is examined in detail to verify the coexistence of multiple luminescent centers. Furthermore, the occupied rates of Eu^{2+} in five sites of CNP:0.1Eu^{2+} suggest that Eu^{2+} enters into Ca(1), Ca(2), Ca(3), and M(4) sites, answering for the two emission bands. By combining the drastic changes of M−O bond length and Eu^{2+} emission by varying the M ions, the distribution of Eu^{2+} ions in $Ca_{10}M(PO_4)_7$ has been confirmed.

EXPERIMENTAL SECTION

Materials and Preparation Method. $Ca_{10-x}M(PO_4)_7$:xEu^{2+} (M = Li, Na and K; $0.001 \leq x \leq 0.1$) were synthesized by a solid-state reaction. $CaCO_3$ (A.R.), Li_2CO_3 (A.R.), Na_2CO_3 (A.R.), K_2CO_3 (A.R.), $NH_4H_2PO_4$ (A.R.), and Eu_2O_3 (99.99%) were used as raw materials. Stoichiometric amounts of the required cation sources were combined and ground together with a small amount of ethanol using an agate mortar and pestle until the mixtures were almost dry (above 25 min). Mixtures were then shifted to the crucible and preheated at 800 °C for 3 h. After being ground, the powder mixtures were sintered again at 1350 °C for 4 h under a reducing atmosphere of N_2−H_2 (5%). After firing, the samples were cooled to room temperature in the furnace and were ground again.

Characterization. Powder X-ray diffraction (XRD) measurements were performed on a D8 Advance diffractometer (Bruker Corporation, Germany), operating at 40 kV and 35 mA with Cu Ka radiation (λ = 1.5406 Å). The scanning rate for phase identification was fixed at 8° min^{-1} with a 2θ range from 15° to 60°, and the data for the Rietveld analysis were collected in a step-scanning mode with a step size of 0.02° and 5 s counting time per step over a 2θ range from 5° to 120°. Synchrotron powder X-ray diffraction (SXRD) data were collected at TPS 09A (Taiwan Photon Source) of the National Synchrotron Radiation Research Center and using an X-ray wavelength of 0.82656 Å. The 15 keV X-ray source is delivered from an in-vacuum undulator (IU22), and the powder diffraction patterns were recorded by a position-sensitive detector, MYTHEN 24K, covering a 2θ range of 120°. The powder sample was loaded into a 0.5 mm capillary for uniform absorption and faster rotation during data collection. Due to the small gaps between detector modules, the two data sets were collected 2° apart with 60 s exposure time, and the data were merged and gridded to give a continuous data set. Rietveld refinement was performed by using TOPAS 4.2.[30] The room-temperature photoluminescence (PL) and photoluminescence excitation (PLE) spectra were carried out by a fluorescence spectrophotometer (F-4600, HITACHI, Japan) equipped with a photomultiplier tube operating at 400 V and a 150 W xenon lamp as the excitation source. The low-temperature luminescence properties were measured on a FLSP9200 fluorescence spectrophotometer (Edinburgh Instruments Ltd., U.K.). The luminescence decay curves were also obtained using a FLSP9200 fluorescence spectrophotometer (Edinburgh Instruments Ltd., U.K.), and an nF900 flash lamp was used as the excitation resource.

RESULTS AND DISCUSSION

Many previous researchers have described the crystal structure of β-$Ca_3(PO_4)_2$, which can be also written as β-$Ca_{21}(PO_4)_{14}$, and when two univalent metals M^+ ions (M = Li, Na, and K) are substituted for one divalent Ca^{2+} ion, β-$Ca_{20}M_2(PO_4)_{14}$ host can be obtained, namely, $Ca_{10}M(PO_4)_7$. Therefore, $Ca_{10}M(PO_4)_7$ is assigned to the β-$Ca_3(PO_4)_2$-type structure in this work. In the $Ca_{10}M(PO_4)_7$ host, there are five independent cation sites, named as Ca(1), Ca(2), Ca(3), M(4), and Ca(5) sites, respectively. All sites are 100% occupied by Ca ions or M ions. Figure S1a (in the Supporting Information) shows the XRD pattern of $Ca_{9.9}M(PO_4)_7$:0.1Eu^{2+} (M = Li, Na, and K), and the results indicate that all peaks of the samples can be well ascribed to a trigonal (*R*3*c*) phase $Ca_{10}K(PO_4)_7$ (JCPDS card no.45-0138). Moreover, Rietveld analysis of the selected chemical compositions of $Ca_{9.9}Li(PO_4)_7$:0.1Eu^{2+} (abbreviated to CLP hereafter), $Ca_{9.9}Na(PO_4)_7$:0.1Eu^{2+} (abbreviated to CNP hereafter), and $Ca_{9.9}Li(PO_4)_7$:0.1Eu^{2+} (abbreviated to CKP hereafter) samples have been conducted, and the results, as shown in Figure S1b−d, also verified that the three phases were isostructural with β-$Ca_3(PO_4)_2$-type structure. The crystallographic parameters obtained from XRD Rietveld refinements for the $Ca_{9.9}M(PO_4)_7$:0.1Eu^{2+} (M = Li, Na, and K) samples are summarized in Table S1. Given that the ion radius of alkali metal (Li, Na, and K) is Li < Na < K, the lattice expansion should take place compared to the peaks of CLP. The dependence of the lattice parameters (*a* and *c*) and cell volume (v) on the ionic radius of M in $Ca_{9.9}M(PO_4)_7$:0.1Eu^{2+} (Li, Na, and K) is shown in Figure 1. It can be seen that lattice parameter *a* and cell volume *V* increase depending on different cations from Li to Na and K. However, the lattice parameter *c* decreases. The reason is associated with special rotation of polyhedra. Herein, if two polyhedras MO_n have a joint O ion and the M−O−M angle is big (>150−160°), then under heating the bond length M−O become bigger, and it leads to the M−O−M angle decreasing. This process looks like rotation of these two polyhedra in different directions. The most important thing is that the

DOI: 10.1021/acs.chemmater.7b02724
Chem. Mater. 2017, 29, 7563−7570

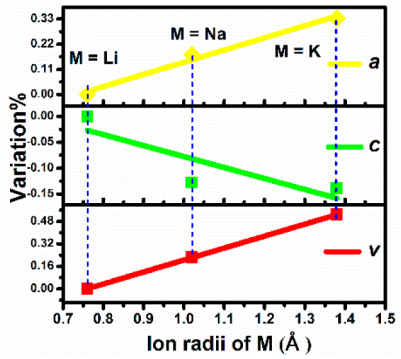

Figure 1. Dependence of the lattice parameters (a and c) and unit cell volume (v) on the ionic radius of Li, Na, and K in $Ca_{9.9}M(PO_4)_7$:$0.1Eu^{2+}$.

distance between M···M becomes smaller and the cell parameters decreased. As we find that the heating process leads to a decrease of the cell parameter and sometimes the cell volume, similarly doping by a bigger ion has the same effect as the heating process, so that the reason for contraction of cell parameters can be similar.

To further investigate how the substitution of different alkali metal ions (Li, Na, and K) affects the $Ca_{10}M(PO_4)_7$:Eu^{2+} luminescent properties, the excitation and emission spectra of $Ca_{10}M(PO_4)_7$:$0.001Eu^{2+}$ (M = Li, Na, and K) are recorded and their comparisons are given in Figure 2, along with the inset photographs of the samples under 365 nm UV lamp irradiation. Additionally, the influence of Eu^{2+} concentration on the luminescence properties of $Ca_{10}M(PO_4)_7$ is also investigated by varying the Eu^{2+} content between 0.001 and 0.08. Figure 2a,b exhibits the normalized excitation spectra and emission spectra of the CLP samples with the different Eu^{2+} concentrations (x = 0.001, 0.005, 0.01, 0.03, 0.05, and 0.08). Upon the increasing of x, there is always one dominating emission band centered at 414 nm with a narrow bandwidth when monitored at 276 nm. However, the origin of a very weak hump in the range of 480−600 nm will be discussed later. Furthermore, the emission intensities have an obvious increasing trend with increasing Eu^{2+} concentration, and then the emission intensity declines dramatically due to the concentration quenching. From the normalized excitation spectra as presented in Figure 2a, it can be seen that the dominant excitation band of Eu^{2+} is located at about 276 nm.

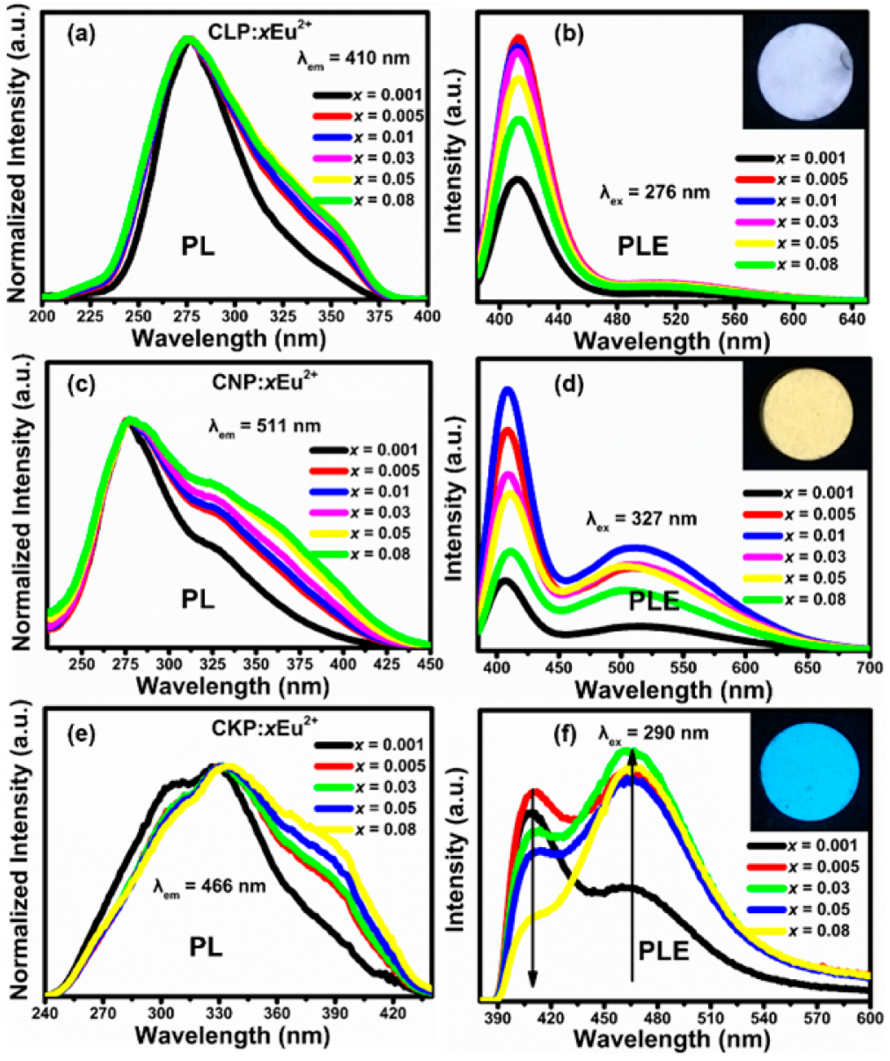

Figure 2. Normalized excitation spectra and emission spectra of $Ca_{10-x}M(PO_4)_7$:xEu^{2+} (M = Li, Na, and K) ($0.001 \leq x \leq 0.08$) samples: (a, b) M = Li, (c, d) M = Na, and (e, f) x = K. Inset: photographs of three samples upon excitation at 365 nm.

DOI: 10.1021/acs.chemmater.7b02724
Chem. Mater. 2017, 29, 7563−7570

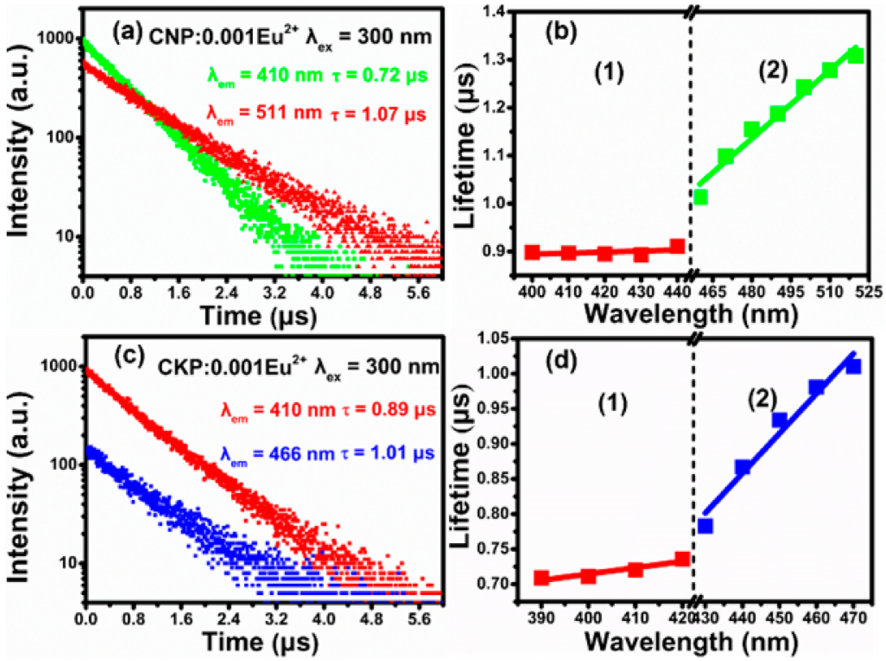

Figure 3. Decay curves of Eu^{2+} in CNP:0.001Eu^{2+} recorded for λ_{ex} = 300 nm and λ_{em} = 410 and 510 nm (a). Dependence of the lifetime values on different monitoring wavelengths λ_{em} = 400−520 nm (b). The decay curves of Eu^{2+} in CKP:0.001Eu^{2+} recorded for λ_{ex} = 300 nm and λ_{em} = 410 and 466 nm (c). Dependence of the lifetime values on different monitoring wavelengths λ_{em} = 390−470 nm (d).

However, additional excitation band centered at 355 nm in the low energy side emerges accompanied by increasing x, but the intensity is weak. As can be seen from the normalized excitation spectra and emission spectra of CNP:$x$$Eu^{2+}$ (x = 0.001, 0.005, 0.01, 0.03, 0.05, and 0.08) in Figure 2c,d, even if the Eu^{2+} content is 0.001, there are two distinct emission bands located at 410 and 511 nm, respectively, in the range of 380−650 nm recorded for λ_{ex} = 327 nm. The emission intensities of two bands first increased and then decreased as a function of x. As shown in Figure 2c, it can be seen that the normalized excitation spectra of CNP:$x$$Eu^{2+}$ consists of two bands within the scope of 250−450 nm, and the main band is centered at 276 nm and the other shoulder on the low energy side of the spectrum is located at 327 nm. Figure 2e,f shows the normalized excitation spectra and emission spectra of CKP:$x$$Eu^{2+}$ (x = 0.001, 0.005, 0.03, 0.05, and 0.08). Under excitation at 290 nm, it also gives two emission bands centered at 410 and 466 nm, respectively. With the increasing of Eu^{2+} concentration, the emission intensity of the shorter-wavelength side at 410 nm decreases gradually together with the gradual increase of the longer-wavelength side at 466 nm, which will also be discussed later. The excitation spectra of CKP:$x$$Eu^{2+}$ contain three peaks centered at 290, 327, and 385 nm, respectively. Comparing to their emission spectra of CLP:0.001Eu^{2+}, CNP:0.001Eu^{2+}, and CKP:0.001Eu^{2+}, for the emission spectra of CLP:0.001Eu^{2+} the 410 nm band dominates. However, the emission spectra of CNP:0.001Eu^{2+} and CKP:0.001Eu^{2+} contain two obvious broad bands. Therefore, we can conclude that the emission band located at 410 nm is intrinsic for the three samples under investigation; however, the second emission band differs in position from CNP:0.001Eu^{2+} and CKP:0.001Eu^{2+} (511 and 466 nm). Possibly the two emission bands in the CNP:0.001Eu^{2+} and CKP:0.001Eu^{2+} indicate that Eu^{2+} ions enter into different crystallographic sites corresponding to different luminescence centers.

As mentioned above, there are five independent crystallographic sites in $Ca_{10}M(PO_4)_7$. From Rietveld refinement analysis for the as-prepared samples, the coordinated number is seven for Ca(1), six for Ca(2), seven for Ca(3), six for M(4), and six for Ca(5), and the average bond length of five sites in the CLP:0.1Eu^{2+}, CNP:0.1Eu^{2+}, and CKP:0.1Eu^{2+} are shown in Table S2. For the Ca(5) site the average bond lengths are 2.26, 2.24, and 2.28 Å corresponding to CLP, CNP, and CKP. Small Ca−O bond length implies that it is unsuitable for doping Eu^{2+}. However, the average bond length of Ca(1), Ca(2), Ca(3), and M(4) sites is big enough for Eu^{2+}. The ionic radii of M ions (in six coordination) are 0.76 Å for Li^+, 1.02 Å for Na^+, 1.38 Å for K^+, and 1.17 Å for Eu^{2+}. In CLP:Eu^{2+} (only a dominated 410 nm band), even if the Li−O bond length is relatively bigger (2.54 Å), we suppose that the Eu^{2+} ions will not prefer to enter the M(4) site owing to the charge mismatch and ion radius mismatch. Thus, Eu^{2+} ions are potentially distributed over Ca(1), Ca(2), and Ca(3) sites. For CNP and CKP, Eu^{2+} ions can occupy Ca(1), Ca(2), Ca(3), and M(4) sites due to no definite limits.

A well-established method to certify the existence of different Eu^{2+} luminescence centers is to measure the luminescence lifetime of CNP:0.001Eu^{2+} and CKP:0.001Eu^{2+} recorded for λ_{ex} = 300 nm, and different emission wavelengths are depicted in Figure 3.[31] As different luminescence centers set in, the luminescence lifetime changes greatly because of an additional nonradiative contribution to the decay process.[32] As an example, luminescence decay curves of CNP:0.001Eu^{2+} were monitored at different detection wavelengths, and the representative decay curves monitored at 410 and 511 nm are presented in Figure 3a. All decay curves are (close to) single exponential. In Figure 3b the lifetimes are plotted as a function of different monitoring wavelengths. Some remarkable differences of the lifetimes increasing suddenly are observed. The lifetimes are evaluated to be 0.72 and 1.07 μs for peaks at 410 and 511 nm, respectively. The above results suggest there are

DOI: 10.1021/acs.chemmater.7b02724
Chem. Mater. 2017, 29, 7563−7570

different luminescence centers in CNP:Eu^{2+}. Furthermore, the lifetimes and decay curves of CKP:0.001Eu^{2+} recorded different wavelengths are depicted in Figure 3c,d. The lifetimes also change greatly, verifying two different luminescence centers.

To accurately find sites which are occupied by Eu^{2+}, the high-quality synchrotron powder pattern of CNP:0.1Eu^{2+} is measured. The Rietveld refinement is accomplished for CNP:0.1Eu^{2+} phosphor from the observed SXRD patterns (Figure 4a), and the final converged weighted profile of R_{wp} is

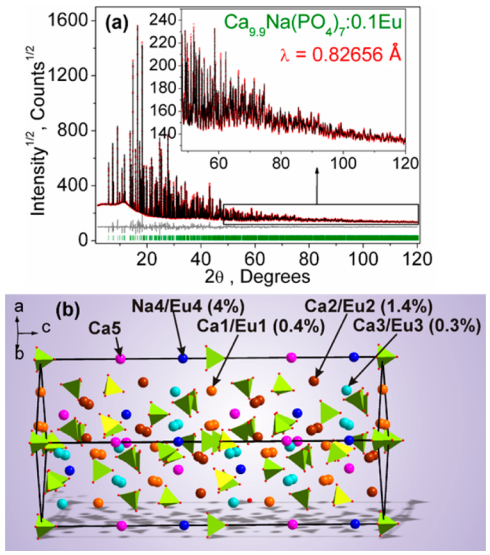

Figure 4. SXRD profile for Rietveld refinement result of CNP:0.1Eu^{2+} (a). Crystal structure of CNP:0.1Eu^{2+} and the occupied rates of Eu^{2+} in Ca(1), Ca(2), Ca(3), Na(4), and Ca(5) sites (b).

4.45%. The refined model shows that the occupied rates of Eu^{2+} in Ca(1), Ca(2), Ca(3), Na(4), and Ca(5) sites are 0.4%, 1.4%, 0.3%, 4%, and 0%, respectively (Table S4). So we can conclude that only four sites are occupied by Eu^{2+}, and the results certify the above result that Eu^{2+} cannot enter into the Ca(5) site. It should be noted that the Na site has the biggest volume over all five sites with an average bond length of d(Na−O) = 2.78 Å, and accordingly it contains the largest amount of Eu^{2+} ions (4%). Figure 4b gives the exact crystal structure of CNP:0.1Eu^{2+} and the Ca/Na atomic site with their corresponding neighboring atoms from the refined results. The precise Rietveld refinement data from the high-quality synchrotron pattern demonstrates the direct evidence from the solid state structure on the different distributions of Eu^{2+} dopant in various crystallographic sites, which is also in agreement with the optical measurement.

Now that there are four cation sites, generally forming four kinds of emission centers in CNP:Eu^{2+} and CKP:Eu^{2+}, the numbers of observed luminescence peaks should be equivalent to the number of sites occupied by the luminescent center ions. Actually only two bands are observed in Figure 2d,f. For CNP, the average Ca/Na−O bond lengths in the Ca(1), Ca(2), and Ca(3) sites are 2.51, 2.49, and 2.52 Å, which are much shorter than the Na−O bond length 2.78 Å (Table S2). The average Ca−O bond lengths of three sites are similar, indicating the similar local environment surrounding Eu^{2+} ions. The Eu^{2+} emission spectra are expected to be similar. Therefore, the four luminescence centers can be divided into two types: (1) Eu^{2+} occupies the Ca(1), Ca(2), and Ca(3) sites, and (2) Eu^{2+} occupies the Na(4) site, respectively. The occupied rates of Eu^{2+} in the four sites also confirm this division, and why only two emission bands were included can be explained. The above analysis also can be suitable for that of the CKP:Eu^{2+}.

Comparing to the host of CLP, CNP, and CKP, the difference is that the ionic radii of Li, Na, and K follow Li < Na < K. Turning to the influence of Li, Na, and K on the emission spectra, as shown in Figure 5a, it is found that the emission

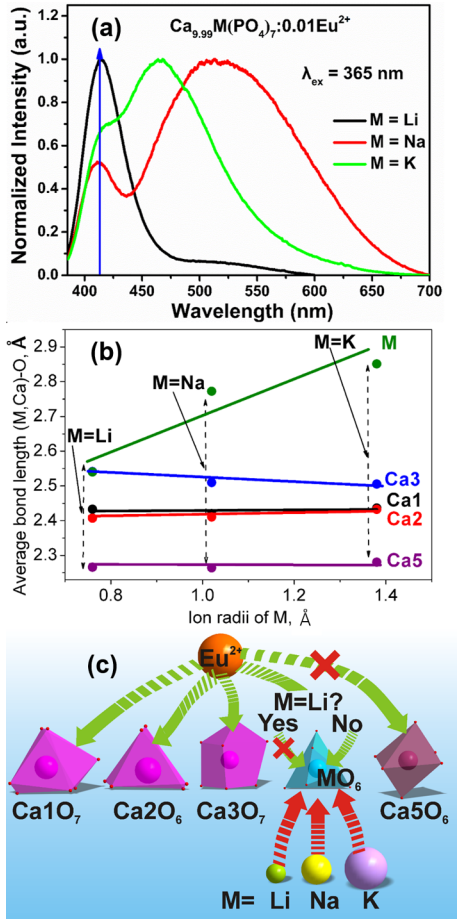

Figure 5. Comparison of the normalized emission spectra of $Ca_{9.99}M(PO_4)_7$:0.01Eu^{2+} (M = Li, Na, and K) samples (a). Main average bond lengths (Å) of five sites in $Ca_{9.9}M(PO_4)_7$:0.1Eu^{2+} as a function of ion radii of M (b). The proposed model on the specific distribution of Eu^{2+} ions in different sites of $Ca_{10}M(PO_4)_7$ host (c).

spectra of the $Ca_{10}M(PO_4)_7$:Eu^{2+} contains the same band at 410 nm, but the second band on the long wavelength side only can be observed as M = Na and K, as also mentioned above. The CLP:Eu^{2+} with a 410 nm band further confirms that the Eu^{2+} cannot enter into the Li(4) site in principle because of the smallest crystallographic site in the CLP host. However, as mentioned above in Figure 2, we should also mention that there is a very weak hump in the emission peak of CLP:Eu^{2+}, which should be possibly related with the occupation of a very small amount of Eu^{2+} in the distorted Li(4) site owing to the elastic lattice and the possibility in statistics.

The average bond lengths of five sites in $Ca_{10}M(PO_4)_7$ as a function of ion radii of M are exhibited in Figure 5b. The differences of the M−O bond lengths, d(Li−O) < d(Na−O) < d(K−O), are remarkable when varying the M ions. However, the average bond lengths of Ca1−O, Ca2−O, and Ca3−O

DOI: 10.1021/acs.chemmater.7b02724
Chem. Mater. 2017, 29, 7563−7570

almost remain the same. Therefore, the variation from Li to Na to K ions only changes the local environment of Eu^{2+} ions in the Na(4) and K(4) sites, which leads to different Eu^{2+} emission in CNP and CKP, as shown in Figure 5a. However, the local environment of Eu^{2+} ions in the Ca(1), Ca(2), or Ca(3) sites remains nearly invariable, so that the Eu^{2+} emission should be the same. Anyway, based on the comparison of the changes of bond-length data and Eu^{2+} luminescence in $Ca_{10}M(PO_4)_7$:Eu^{2+}, we propose a model for specific distribution of Eu^{2+} ions in different sites: the emission band around 410 nm is originated from Eu^{2+} ions that are distributed over Ca(1), Ca(2), and Ca(3) sites, while the emission band on the long wavelength side (511 and 466 nm) is attributed to the Eu^{2+} ions that enter the M(4) site (M = Na and K). To further validate our speculation, two solid solutions of $Ca_{10}Li_{0.2}Na_{0.5}K_{0.3}(PO_4)_7$:$Eu^{2+}$ and $Ca_{10}Na_{0.6}K_{0.4}(PO_4)_7$:$Eu^{2+}$ are designed to provide better insight into understanding the crystallography occupied. Provided that, the 410 nm emission band is assigned to Eu^{2+} ions that enter the M(4) site, while the other band is owing to that Eu^{2+} occupy one Ca(1)−Ca(3) sites. When Li, Na, and K ions are introduced into one phase, theoretically the emission spectra of the designed $Ca_{10}Li_{0.2}Na_{0.5}K_{0.3}(PO_4)_7$:$Eu^{2+}$ should consist of three bands (410, 466, and 511 nm). Actually, as can be seen from the emission spectra of two solid solutions (Figure S2), they both consist of two bands centered at ∼410 nm and ∼500 nm. This result proves the above assumption is invalid and further confirms that the model for crystallographic occupation of Eu^{2+} we proposed is reasonable in $Ca_{10}M(PO_4)_7$:Eu^{2+} (M = Li, Na, and K), as shown in Figure 5c.

Additionally, the second emission bands of CNP:0.01Eu^{2+} and CKP:0.01Eu^{2+} are located at 511 and 466 nm, respectively. The shift to higher energies of the second emission from Na to K is due to the crystal field splitting (Dq), and it is expressed as follows:[33]

$$Dq = \frac{ze^2r^4}{6R^5} \quad (1)$$

where Dq is the measurement of the crystal field strength, R is the distance between the central ion and its ligands, z is the charge or valence of the anion, e is the charge of an electron, and r is the radius of the d wave function. The bond length K−O is bigger than that of Na−O, and it leads the crystal field splitting becoming smaller, while the position of the lowest energy 5d state (the emitting state) shifts to higher energies. Thus, a blue shift can be observed. These results further confirm that the second emission band located at 511 or 466 nm is attributed to Eu^{2+} ions that enter M(4) (M = Na and K). Furthermore, according to the above discussion, the four crystallographic sites can be occupied by Eu^{2+}, and two sets of luminescence centers have different surrounding environments; the emission band around 410 nm is ascribed to the Eu^{2+} ions that are distributed over the Ca(1), Ca(2), and Ca(3) sites, which have similar surrounding environments. To distinguish the difference among the three sites, the excitation and emission spectra of CKP:0.001Eu^{2+} are recorded at 80 K as shown in Figure S3, which reflect the intrinsic luminescence properties of the isolated Eu^{2+}. However, no obvious differences are observed in the emission spectra monitored at different excitation wavelengths. This suggests that the emitting d-levels for the three sites are too close in energy to be clearly distinguished, even at low temperature.[34]

To understand the correlation of different emission centers, it is worth noting that the 410 nm emission band of CKP:$x$$Eu^{2+}$ is dominant for x = 0.001 and then the emitting intensities of both bands (410 and 466 nm) are enhanced as x = 0.005 (shown in Figure 2f). It is assigned to preferential site occupation of Eu^{2+} in different crystallographic sites. At low Eu^{2+} concentration, Eu^{2+} prefers to occupy the Ca(1), Ca(2), and Ca(3) sites and affords the emission band at 410 nm, named the Eu(I) luminescence center. For higher amounts of Eu^{2+}, Eu^{2+} enters into the K(4) site preferentially, named the Eu(II) luminescence center, which is responsible for the emission band at 466 nm. For x > 0.005, the intensity of the emission band at 410 nm decreases, and the emitting intensity of the 466 nm band strengthens and becomes the dominant emission. A possible cause for the phenomenon is related to the energy transfer behaviors among different Eu^{2+} sites due to the presence of two luminescence centers (Eu(I) and Eu(II)). In the case of energy transfer, there are additional decay channels that shorten the lifetime of the excited state.[34] Therefore, to determine if the energy transfer is responsible, the concentration dependence of the luminescence lifetime, monitored at λ_{em} = 410 and 466 nm, is considered. Figure 6 shows the decay curves and lifetime values of Eu(I) and Eu(II) in CKP as a function of x. As can be seen from the variation of lifetime values in different emission centers (Figure 6c), the values for both of the two emission centers are shortened obviously upon increasing the Eu^{2+} concentration, especially for the shorter wavelength side of the emission band (410 nm). The above results indicate that the intensity changes between two bands (410 and 466 nm) in the CKP:$x$$Eu^{2+}$ are caused by energy transfer from Eu(I) to Eu(II).

CONCLUSIONS

In summary, we presented a crystal-site engineering approach to probe the Eu^{2+} luminescence in different crystallographic sites of $Ca_{10}M(PO_4)_7$ (M = Li, Na, and K) and realize photoluminescence tuning from bluish-violet to blue and yellow. Eu^{2+} emission in CLP gives one dominated peaks at about 410 nm, while two emission bands can be observed in CNP:Eu^{2+} (410 and 511 nm) and CKP:Eu^{2+} (410 and 466 nm), respectively. The variation in decay rate with respect to different detection wavelengths has verified the coexistence of multiple luminescent centers in $Ca_{10}M(PO_4)_7$:Eu^{2+}. The Rietveld refinement using synchrotron powder diffraction data confirms the different occupied rates of Eu^{2+} in the Ca(1), Ca(2), Ca(3), Na(4), and Ca(5) sites of $Ca_{10}Na(PO_4)_7$. The influence of Li, Na, and K on the Eu^{2+} luminescence and average bond-length d(M−O) provide insight to probe the distribution of Eu^{2+} ions from another insight into the distribution of the crystallographic sites. Combing the drastic changes of the d(M−O) bond length (d(Ca−O) almost stays the same in three sites) and Eu^{2+} emission, we confirm that the emission band at 410 nm is due to the distribution of Eu^{2+} in the Ca(1), Ca(2), and Ca(3) sites with similar local structures, while the long-wavelength band (466 or 511 nm) is attributed to the Eu^{2+} that enters the M(4) site (M = Na and K). The blue-shift (511 to 466 nm) of the second emission peak is due to the crystal field splitting by varying from Na to K in M(4) sites. These results demonstrate that the crystal-site engineering approach can control the distribution of the RE dopants in the solid state compounds and open a new gate for the photoluminescence tuning and optimization.

DOI: 10.1021/acs.chemmater.7b02724
Chem. Mater. 2017, 29, 7563−7570

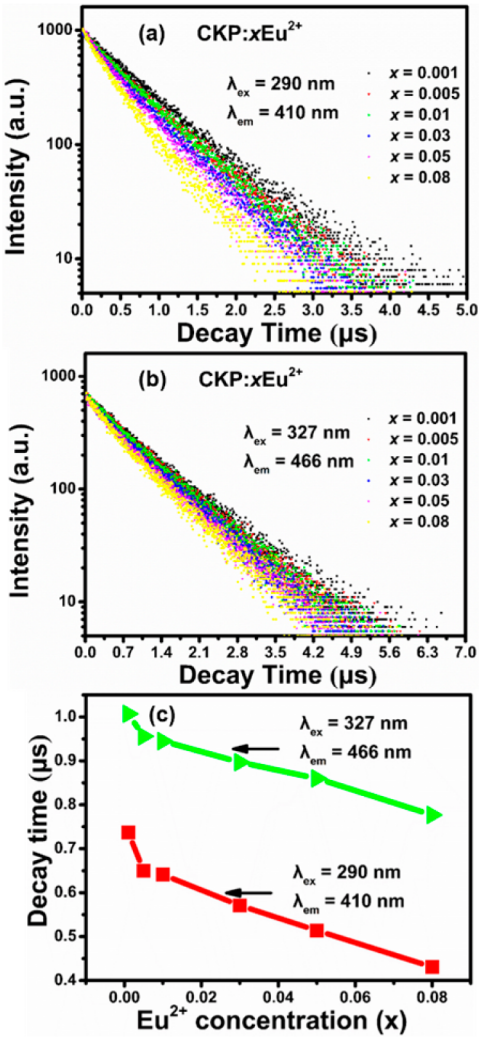

Figure 6. Decay curves of the defined Eu(I) (a) and Eu(II) (b) emission centers in CKP:xEu^{2+} as a function of x and the dependence of the lifetime values of Eu(I) and Eu(II) on different Eu^{2+} concentrations in CKP:xEu^{2+} (c).

■ ASSOCIATED CONTENT

Supporting Information

The Supporting Information is available free of charge on the ACS Publications website at DOI: 10.1021/acs.chemmater.7b02724.

XRD patterns, Rietveld analysis, emission spectra (at room temperature), and excitation and emission spectra (at 80 K) appear in Figures S1−S3; structural data and average bond lengths are given in Table S1−S4 (PDF)

■ AUTHOR INFORMATION

Corresponding Author

*E-mail: xiazg@ustb.edu.cn (Z. Xia).

ORCID

Zhiguo Xia: 0000-0002-9670-3223

Quanlin Liu: 0000-0003-3533-7140

Notes

The authors declare no competing financial interest.

■ ACKNOWLEDGMENTS

The present work was supported by the National Natural Science Foundation of China (Grants 51722202, 91622125, and 51572023), Natural Science Foundations of Beijing (2172036), and Fundamental Research Funds for the Central Universities (FRF-TP-16-002A3). C.C.L. and C.C.S. acknowledge the financial support from the Ministry of Science and Technology of Taiwan (Contract No. MOST 104-2113-M-027-007-MY3), and M. Molokeev acknowledges support of the Russian Foundation for Basic Research (17-52-53031).

■ REFERENCES

(1) George, N. C.; Denault, K. A.; Seshadri, R. Phosphors for solid-state white lighting. *Annu. Rev. Mater. Res.* **2013**, *43*, 481−501.

(2) Xia, Z. G.; Liu, Q. L. Progress in discovery and structural design of color conversion phosphors for LEDs. *Prog. Mater. Sci.* **2016**, *84*, 59−117.

(3) Seibald, M.; Rosenthal, T.; Oeckler, O.; Maak, C.; Tücks, A.; Schmidt, P. J.; Wiechert, D.; Schnick, W. New polymorph of the highly efficient LED-phosphor $SrSi_2O_2N_2$:Eu^{2+}- polytypism of a layered oxonitridosilicate. *Chem. Mater.* **2013**, *25*, 1852−1857.

(4) Song, E. H.; Wang, J. Q.; Shi, J. H.; Deng, T. T.; Ye, S.; Peng, M. Y.; Wang, J.; Wondraczek, L.; Zhang, Q. Y. Highly efficient and thermally stable K_3AlF_6:Mn^{4+} as a red phosphor for ultra-high-performance warm white light-Emitting diodes. *ACS Appl. Mater. Interfaces* **2017**, *9*, 8805−8812.

(5) Kang, F.; Zhang, Y.; Peng, M. Y. Controlling the energy transfer via multi luminescent centers to achieve white light/tunable emissions in a single-phased X2-type Y_2SiO_5:Eu^{3+},Bi^{3+} phosphor for ultraviolet converted LEDs. *Inorg. Chem.* **2015**, *54*, 1462−73.

(6) Chen, Y.; Li, Y.; Wang, J.; Wu, M. M.; Wang, C. X. Color-tunable phosphor of Eu^{2+} and Mn^{2+} codoped $Ca_2Sr(PO_4)_2$ for UV light-emitting diodes. *J. Phys. Chem. C* **2014**, *118*, 12494−12499.

(7) Xia, Z. G.; Liu, H. K.; Li, X.; Liu, C. Y. Identification of the crystallographic sites of Eu^{2+} in $Ca_9NaMg(PO_4)_7$: structure and luminescence properties study. *Dalton Trans.* **2013**, *42*, 16588−16595.

(8) Ji, H. P.; Huang, Z. H.; Xia, Z. G.; Molokeev, M. S.; Atuchin, V. V.; Fang, M. H.; Liu, Y. G. Discovery of new solid solution phosphors via cation substitution-dependent phase transition in $M_3(PO_4)_2$:Eu^{2+} (M= Ca/Sr/Ba) quasi-binary sets. *J. Phys. Chem. C* **2015**, *119*, 2038−2045.

(9) Belik, A.; Izumi, F.; Stefanovich, S. Y.; Malakho, A.; Lazoryak, B.; Leonidov, I.; Leonidova, O.; Davydov, S. Polar and Centrosymmetric Phases in Solid Solutions $Ca_{3-x}Sr_x(PO_4)_2$ ($0 \le x \le 16/7$). *Chem. Mater.* **2002**, *14*, 3197−3205.

(10) Ji, H. P.; Huang, Z. H.; Xia, Z. G.; Molokeev, M. S.; Atuchin, V. V.; Fang, M. H.; Huang, S. F. New yellow-emitting whitlockite-type structure $Sr_{1.75}Ca_{1.25}(PO_4)_2$:Eu^{2+} phosphor for near-UV pumped white light-emitting devices. *Inorg. Chem.* **2014**, *53*, 5129−5135.

(11) Morozov, V. A.; Belik, A. A.; Kotov, R. N.; Presnyakov, I. A.; Khasanov, S. S.; Lazoryak, B. I. Crystal structures of double calcium and alkali metal phosphates $Ca_{10}M(PO_4)_7$(M = Li, Na, K). *Crystallogr. Rep.* **2000**, *45*, 13−20.

(12) Wang, J.; Zhang, Z. Y.; Zhang, M.; Zhang, Q. H.; Su, Q.; Tang, J. K. The energy transfer from Eu^{2+} to Tb^{3+} in $Ca_{10}K(PO_4)_7$ and its application in green light emitting diode. *J. Alloys Compd.* **2009**, *488*, 582−585.

(13) Zhao, J. W.; Wu, Y.; Liang, Y. J.; Liu, M. Y.; Yang, F.; Xia, Z. G. A novel green-emitting phosphor $Ca_{10}Na(PO_4)_7$:Eu^{2+} for near ultraviolet white light-emitting diodes. *Opt. Mater.* **2013**, *35*, 1675−1678.

(14) Wang, Y.; Li, H.; Zhang, R.; Zhan, M.; Zhang, J. Investigations on the luminescence of emission-tunable $Ca_{10}K(PO_4)_7$:Eu^{2+},Sr^{2+},Mg^{2+} phosphors for white LEDs. *RSC Adv.* **2015**, *5*, 2689−2693.

(15) Huang, C. H.; Chen, T. M. $Ca_9La(PO_4)_7$:Eu^{2+},Mn^{2+}: an emission-tunable phosphor through efficient energy transfer for white light-emitting diodes. *Opt. Express* **2010**, *18*, 5089−5099.

DOI: 10.1021/acs.chemmater.7b02724
Chem. Mater. 2017, 29, 7563−7570

(16) Guo, N.; You, H. P.; Song, Y. H.; Yang, M.; Liu, K.; Zheng, Y. H.; Huang, Y. J.; Zhang, H. J. White-light emission from a single-emitting-component $Ca_9Gd(PO_4)_7:Eu^{2+},Mn^{2+}$ phosphor with tunable luminescent properties for near-UV light-emitting diodes. *J. Mater. Chem.* **2010**, *20*, 9061−9067.
(17) Zatovsky, I. V.; Strutynska, N. Y.; Baumer, V. N.; Shishkin, O. V.; Slobodyanik, N. S. The whitlockite-related phosphate $Ca_9Cr(PO_4)_7$. *Acta Crystallogr., Sect. E: Struct. Rep. Online* **2007**, *63*, i180−i181.
(18) Benhamou, R. A.; Bessière, A.; Wallez, G.; Viana, B.; Elaatmani, M.; Daoud, M.; Zegzouti, A. New insight in the structure-luminescence relationships of $Ca_9Eu(PO_4)_7$. *J. Solid State Chem.* **2009**, *182*, 2319−2325.
(19) Wen, D. W.; Dong, Z. Y.; Shi, J. X.; Gong, M. L.; Wu, M. M. Standard white-emitting $Ca_8MgY(PO_4)_7:Eu^{2+},Mn^{2+}$ phosphor for white-light-emitting LEDs. *ECS J. Solid State Sci. Technol.* **2013**, *2*, R178−R185.
(20) Xue, Y. N.; Xiao, F.; Zhang, Q. Y. A red-emitting $Ca_8MgLa(PO_4)_7:Ce^{3+},Mn^{2+}$ phosphor for UV-based white LEDs application. *Spectrochim. Acta, Part A* **2011**, *78*, 1445−1448.
(21) Huang, Y. L.; Ding, H. Y.; Jang, K. W.; Cho, E. J.; Lee, H.; Jayasimhadri, M.; Yi, S.-S. Luminescence properties of triple phosphate $Ca_8MgGd(PO_4)_7:Eu^{2+}$ for white light-emitting diodes. *J. Phys. D: Appl. Phys.* **2008**, *41*, 095110.
(22) Guo, N.; Huang, Y. Y.; You, H. P.; Yang, M.; Song, Y. H.; Liu, K.; Zheng, Y. H. $Ca_9Lu(PO_4)_7:Eu^{2+},Mn^{2+}$: a potential single-phased white-light-emitting phosphor suitable for white-light-emitting diodes. *Inorg. Chem.* **2010**, *49*, 10907−10913.
(23) Huang, C. H.; Chen, T. M.; Liu, W. R.; Chiu, Y. C.; Yeh, Y. T.; Jang, S. M. A single-phased emission-tunable phosphor $Ca_9Y(PO_4)_7:Eu^{2+},Mn^{2+}$ with efficient energy transfer for white-light-emitting diodes. *ACS Appl. Mater. Interfaces* **2010**, *2*, 259−264.
(24) Li, G. G.; Tian, Y.; Zhao, Y.; Lin, J. Recent progress in luminescence tuning of Ce^{3+} and Eu^{2+}-activated phosphors for pc-WLEDs. *Chem. Soc. Rev.* **2015**, *44*, 8688−8713.
(25) Sato, Y.; Kato, H.; Kobayashi, M.; Masaki, T.; Yoon, D. H.; Kakihana, M. Tailoring of deep-red luminescence in $Ca_2SiO_4:Eu^{2+}$. *Angew. Chem., Int. Ed.* **2014**, *53*, 7756−9.
(26) Zhang, X. J.; Wang, J.; Huang, L.; Pan, F. J.; Chen, Y.; Lei, B. F.; Peng, M. Y.; Wu, M. M. Tunable Luminescent Properties and Concentration-Dependent, Site-Preferable Distribution of Eu^{2+} Ions in Silicate Glass for White LEDs Applications. *ACS Appl. Mater. Interfaces* **2015**, *7*, 10044−54.
(27) Chen, M. Y.; Xia, Z. G.; Molokeev, M. S.; Wang, T.; Liu, Q. L. Tuning of Photoluminescence and Local Structures of Substituted Cations in $xSr_2Ca(PO_4)_2$-$(1-x)Ca_{10}Li(PO_4)_7:Eu^{2+}$ Phosphors. *Chem. Mater.* **2017**, *29*, 1430−1438.
(28) Yu, H.; Deng, D. G.; Li, Y. Q.; Xu, S. Q.; Li, Y. Y.; Yu, C. P.; Ding, Y. Y.; Lu, H. W.; Yin, H. Y.; Nie, Q. L. Electronic structure and photoluminescence properties of yellow-emitting $Ca_{10}Na(PO_4)_7:Eu^{2+}$ phosphor for white light-emitting diodes. *J. Lumin.* **2013**, *143*, 132−136.
(29) Liu, W. R.; Chiu, Y. C.; Yeh, Y. T.; Jang, S. M.; Chen, T. M. Luminescence and energy transfer mechanism in $Ca_{10}K(PO_4)_7:Eu^{2+},Mn^{2+}$ phosphor. *J. Electrochem. Soc.* **2009**, *156*, J165−J169.
(30) Bruker, A. *TOPAS*, version 3: General profile and structure analysis software for powder diffraction data; User's Manual; Bruker AXS: Karlsruhe, Germany, 2005.
(31) Lu, Z. J.; Mao, Z. Y.; Chen, J. J.; Wang, D. J. Red/blue-shift dual-directional regulation of α'_L-$(Ca,Sr)_2SiO_4:Eu^{2+}$ phosphors resulting from the incorporation content of Eu^{2+}/Sr^{2+} ions. *Dalton Trans.* **2015**, *44*, 15620−15627.
(32) Han, J.; Zhou, W. L.; Qiu, Z. X.; Yu, L. P.; Zhang, J. L.; Xie, Q. J.; Wang, J.; Lian, S. X. Redistribution of Activator Tuning of Photoluminescence by Isovalent and Aliovalent Cation Substitutions in Whitlockite Phosphors. *J. Phys. Chem. C* **2015**, *119*, 16853−16859.
(33) Duan, C.; Reid, M. A simple model for $f \rightarrow d$ transitions of rare-earth ions in crystals. *J. Solid State Chem.* **2003**, *171*, 299−303.
(34) Bachmann, V.; Ronda, C.; Oeckler, O.; Schnick, W.; Meijerink, A. Color point tuning for $(Sr,Ca,Ba)Si_2O_2N_2:Eu^{2+}$ for white light LEDs. *Chem. Mater.* **2009**, *21*, 316−325.

DOI: 10.1021/acs.chemmater.7b02724
Chem. Mater. 2017, 29, 7563−7570